5078–5087 *Nucleic Acids Research, 2012, Vol. 40, No. 11* *Published online 22 February 2012*
doi:10.1093/nar/gks174

Investigating the entire course of telithromycin binding to *Escherichia coli* ribosomes

Ourania N. Kostopoulou[1], Alexandros D. Petropoulos[1], George P. Dinos[1], Theodora Choli-Papadopoulou[2] and Dimitrios L. Kalpaxis[1,*]

[1]Department of Biochemistry, School of Medicine, University of Patras, 26504 Patras and [2]Laboratory of Biochemistry, School of Chemistry, Aristotle University of Thessaloniki, 54006 Thessaloniki, Greece

Received December 5, 2011; Revised January 15, 2012; Accepted February 2, 2012

ABSTRACT

Applying kinetics and footprinting analysis, we show that telithromycin, a ketolide antibiotic, binds to *Escherichia coli* ribosomes in a two-step process. During the first, rapidly equilibrated step, telithromycin binds to a low-affinity site (K_T = 500 nM), in which the lactone ring is positioned at the upper portion of the peptide exit tunnel, while the alkyl–aryl side chain of the drug inserts a groove formed by nucleotides A789 and U790 of 23S rRNA. During the second step, telithromycin shifts slowly to a high-affinity site (K_T* = 8.33 nM), in which the lactone ring remains essentially at the same position, while the side chain interacts with the base pair U2609:A752 and the extended loop of protein L22. Consistently, mutations perturbing either the base pair U2609:A752 or the L22-loop hinder shifting of telithromycin to the final position, without affecting the initial step of binding. In contrast, mutation Lys63Glu in protein L4 placed on the opposite side of the tunnel, exerts only a minor effect on telithromycin binding. Polyamines disfavor both sequential steps of binding. Our data correlate well with recent crystallographic data and rationalize the changes in the accessibility of ribosomes to telithromycin in response to ribosomal mutations and ionic changes.

INTRODUCTION

Macrolide antibiotics represent a large family of polyketide compounds that act as inhibitors of bacterial protein synthesis. They continue to enjoy a remarkable interest within pharmaceutical industry, because many have been already introduced in clinical applications, while others are used as lead compounds in search for new semisynthetic, anti-infectious agents with improved pharmaceutical properties (1). Accumulated biochemical, genetic and crystallographic evidences suggest that macrolides exert their antimicrobial activity by binding to approximately the same region of the large ribosomal subunit, within a hydrophobic crevice of the peptide exit tunnel, situated between the peptidyltransferase (PTase) center and a constriction in the tunnel formed by proteins L4 and L22 (2). By binding to this site, macrolides hinder the progression of the nascent peptide chain through the exit tunnel, which eventually falls off the ribosome as oligopeptidyl-tRNA, in a process called 'drop off' (3). Although macrolides are accommodated within the same binding pocket, their specific interactions with the ribosome might vary in accordance with the idiosyncratic chemical nature of each drug. Tylosin, for instance, processing a mycaminose/mycarose side chain (Figure 1), extends towards the PTase center and, apart from occluding the exit tunnel, inhibits peptide bond formation if the donor tRNA bears a large amino acid (4).

Binding of an antibiotic to the ribosome is a prerequisite for its action. Most of the earlier studies investigating the kinetics of antibiotic interactions with the ribosome operate on the assumption that the interaction between ribosome (R) and antibiotic (I) can be expressed by a fast-equilibrated reaction of the form: $R + I \rightleftharpoons RI$ (5–7). In fact, this concession is not valid for macrolides. As justified by kinetic studies (4,8–12), NMR and modeling studies (13,14), and footprinting analysis at discrete time-intervals following mixing the ribosome with the drugs (4,12), access of macrolides to *Escherichia coli* ribosomes occurs through a two-step process; a first rapidly equilibrated step representing the recognition and selection of macrolides (I) by the ribosome (R), and a second one corresponding to a slow isomerization of the encounter complex (RI) to a final tight complex (R*I). In some cases the binding was found to follow one-step mechanism (3,9). Even in the latter cases, however, the inhibitor retains its slow binding behavior.

*To whom correspondence should be addressed. Tel: +30 2610996124; Fax: +30 2610969167; Email: dimkal@med.upatras.gr

The authors wish it to be known that, in their opinion, the first two authors should be regarded as joint First Authors.

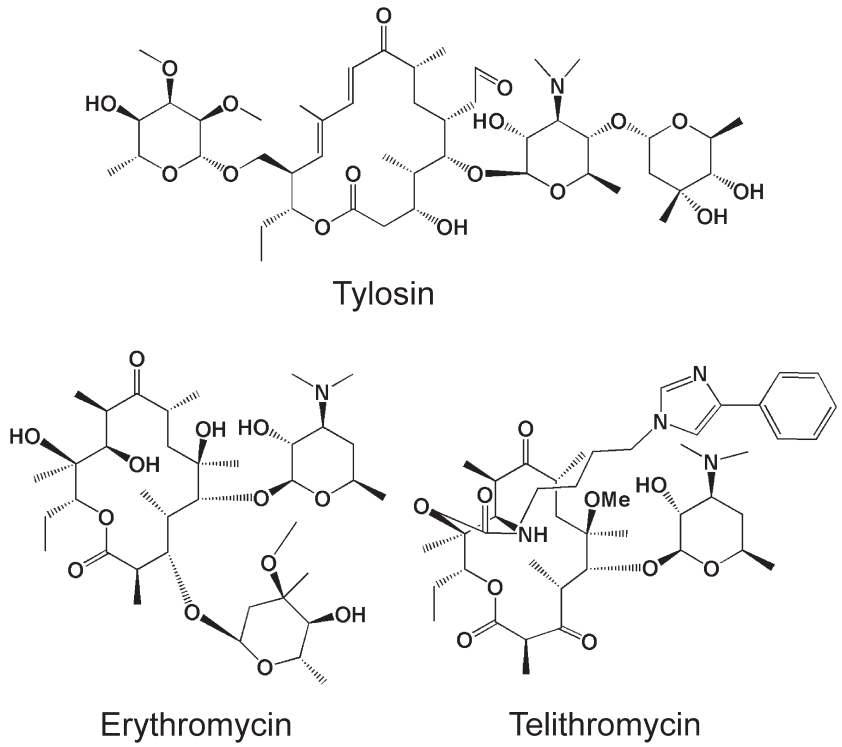

Figure 1. Chemical structures of tylosin, erythromycin and telithromycin.

In an effort to combat the emergence of bacterial resistance to macrolide antibiotics, extensive research on the modification of the prototype macrolide, erythromycin, led to the development of ketolides (15,16). Telithromycin is the first ketolide introduced into clinical practice. It differs from erythromycin by having a keto group at the C-3 position of the lactone ring, instead of the neutral sugar L-cladinose (Figure 1). In addition, telithromycin has the 6-OH of the lactone methylated and possesses an alkyl–aryl arm attached to carbamate heterocycle that involves the C-11 and C-12 positions of the lactone ring. Owing to its more elaborated chemistry, telithromycin compared with erythromycin and other newer macrolides exhibits superior clinical efficacy in upper and lower respiratory tract infections caused by pathogens including strains resistant to macrolides (17). Previous biochemical and genetic studies indicated that, though telithromycin and erythromycin exploit the same high-affinity pocket in the ribosome, the specific interactions of each drug vary in accordance with its chemical nature. Specifically, apart from the interactions between the hydrophobic face of the lactone ring and the G2057–A2059 crevice of the exit tunnel, the binding of telithromycin seems to benefit from interactions of the side chain with U2609 and the loop of helix 35 of 23S rRNA (18–25). In this way, potential interactions of the side chain with ribosomal residues placed deeper in the exit tunnel may compensate for lost of the classical 2058–2059 contacts due to methylation or mutations and gain weight in efficient antibiotic binding. Earlier crystallographic studies of telithromycin in complex with the large ribosomal subunit of *Deinococcus radiodurans* (D50S) and *Haloarcula marismortui* (H50S) failed, each one, to whole verify the mutational and footprinting profile (26,27). In the D50S model, the side chain of telithromycin penetrates deeper into the tunnel and inserts into a groove formed by nucleotides A764 (A751), A802 (A789) and C803 (U790) within domain II of 23S rRNA (terms in parenthesis represent the equivalent residues in *E. coli*). In the H50S model, the side chain is folded across the lactone ring and stacks on nucleotide C2644 (U2609) within domain V of 23S rRNA. Structural and functional studies have demonstrated that cations play a significant role in macrolide–ribosome interactions (4,5,12,28,29). Therefore, apart from species-specific structural ribosomal differences, ionic environment differences between bacterial and archeal ribosomes may conceivably cause an alternative drug conformation (30). Recent crystallographic structures of ribosomes from two eubacteria, *E. coli* and *Thermus thermophilus*, in complex with telithromycin seem to address the disagreements between the *H. marismortui* and *D. radiodurans* structural data (31,32). Nevertheless, crystallographic structures provide only a snapshot of telithromycin binding process and cannot describe the entire course of unique conformations and spatial interactions by which the drug gain access to the tight binding site on the ribosome.

In the present study, kinetic analysis and footprinting analysis at distinct binding-steps are applied to investigate the entire course of telithromycin interaction with wild-type or mutant *E. coli* functional ribosomal complexes, under various ionic conditions. Together

with recent crystallographic data, our results solve previous uncertainties and offer new clues as to how telithromycin seeks out its final position in the ribosome.

MATERIALS AND METHODS

Reagents, materials and strains

Spermine tetrahydrochloride, spermidine trihydrochloride, dimethyl sulfate (DMS), DMS stop solution, puromycin dihydrochloride, tylosin tartrate and $tRNA^{Phe}$ from *E. coli* were provided by Sigma-Aldrich. Kethoxal was from MP Biomedicals, while 1-cyclohexyl-3-(2-morpholinoethyl) carbodiimide metho-*p*-toluene (CMCT) was from Fluka Biochemicals. Radioactive materials were from Amersham Biosciences. AMV reverse transcriptase, dNTPs and ddNTPs were from Roche Diagnostics. Telithromycin was kindly provided by Sanofi-Aventis Inc. Cellulose nitrate filters (type HA; 0.45 μm pore size) were from Millipore Corp. Erythromycin-resistant strains N281 and N282 of *E. coli*, mutated in ribosomal protein L22 (deletion of methionine, lysine and arginine at positions 82–84, here referred to as Δ82–84) and in L4 (a single amino acid substitution at position 63, here referred to as Lys63Glu) (33), respectively, were kindly provided by Dr S.T. Gregory (Brown University). *Escherichia coli* TA531 cells lacking chromosomal *rrn* alleles, but containing pKK35 plasmids possessing wild-type or mutated 23S rRNA (U2609C or U754A) were kindly provided by Dr A.S. Mankin (University of Illinois).

Biochemical preparations

70S ribosomes, Ac[^{3}H]Phe-tRNA charged to 80% and a post-translocation complex of poly(U)-programmed ribosomes, complex C, carrying $tRNA^{Phe}$ at the E-site and Ac[^{3}H]Phe-tRNA at the P-site were prepared as described previously (34). The percentage of complex C, reactive towards puromycin, was >90%.

Kinetics of telithromycin interaction with complex C containing wild-type or mutated ribosomes

As previously proved (4), tylosin inhibits the puromycin reaction, a model reaction for peptide bond formation, since this macrolide possesses a long dissacharide chain extending towards the PTase center and perturbing the positioning of the 3′-end of P-site bound AcPhe-tRNA (Figure 1). Telithromycin does not inhibit the puromycin reaction, however, it competes with tylosin for overlapping binding sites on the ribosome. Taking advantage of this competition, we added complex C into buffer A [100 mM Tris/HCl, pH 7.2, 4.5 mM $Mg(CH_3COO)_2$, 150 mM NH_4Cl, 6 mM β-mercaptoethanol] containing 4 μM tylosin and telithromycin at specified concentrations. The mixture was incubated at 25°C for the desired time intervals and the process of the reaction was monitored by titrating the remaining activity of complex C with puromycin (2 mM, 25°C). In parallel experiments, complex C was pre-incubated with telithromycin for 15 min and then added in the solution of tylosin. Since telithromycin, like erythromycin (4), binds to complex C via two sequential reactions, the first one proceeding much faster than the subsequent isomerization step, the competition between telithromycin (T) and tylosin (I) for complex C can be described by kinetic Scheme 1. Therefore, data processing and calculation of the values of K_T, $k_{on,T}$ and $k_{off,T}$ constants were done in an analogous way to those previously used for kinetic analysis of erythromycin binding (see supplementary material in ref. 4). The dissociation constant K_T*, representing the overall affinity of complex C for telithromycin, was calculated through the relationship (35),

$$K_T^* = K_T\left(\frac{k_{off,}T}{k_{on,}T + k_{off,}T}\right) \quad (1)$$

To estimate the $k_{off,T}$ value by an alternative way and to calculate how many molecules of telithromycin bind per *E. coli* ribosome, complex C*T (10 pmol) absorbed on a cellulose nitrate filter was immersed in 5 ml of buffer A containing 4 μM tylosin for specified time intervals. After removing the excess of tylosin by fast washing with buffer A, the percentage (x) of complex C*T remaining active was titrated with 2 mM puromycin. At dilution, rebinding of telithromycin to ribosomes is negligible, and the rate of dissociation corresponds to the k_{off} of the telithromycin–ribosome complex. Therefore, the $k_{off,T}$ value was estimated from the slope of the obtained semi-logarithmic time plot.

Probing of CT and C*T complexes

Complex C (10 pmol) was incubated in the absence or presence of 2.5 μM telithromycin ($50 \times K_T$) in 100 μl buffer B [50 mM HEPES/KOH, pH 7.2, 4.5 mM $Mg(CH_3COO)_2$, 150 mM NH_4Cl, and 5 mM dithiothreitol] at 25°C, either for 5 s (CT probing) or for $8 \times t_{1/2}$ min (C*T probing). The term $t_{1/2}$ represents the half life for the attainment of equilibrium in complex C interaction with telithromycin and is given by the Equation 2,

$$t_{1/2} = \frac{0.693}{k''} \quad (2)$$

where k'' is the apparent equilibration rate constant, given by Equation 3.

$$k'' = k_{off,T} + k_{on,T}\frac{[T]}{K_T + [T]} \quad (3)$$

Probing of CT and C*T complexes with DMS, kethoxal and CMCT, and monitoring of the modifications in 23S rRNA were performed by primer extension analysis, according to Stern *et al.* (36). Extension products were run on 6% polyacrylamide/7 M Urea gels. Quantification and normalization of band intensities were done as described previously (4). The values indicated in Table 3 denote the ratio between the intensity of a band of interest and the intensity of the corresponding band obtained in the absence of telithromycin.

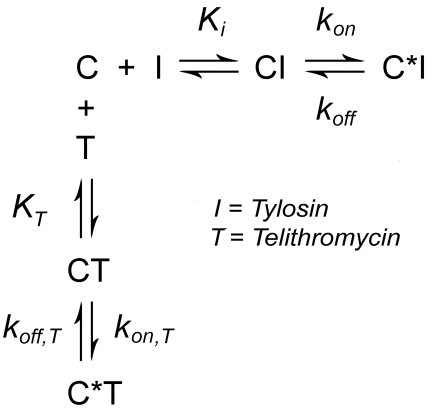

Scheme 1. Competition between telithromycin (T) and tylosin (I) for binding to ribosomal complex C.

Sensitivity to telithromycin of *E. coli* cells containing wild-type or mutant ribosomes

Cells (400 µl of a 0.700 OD_{560} preculture) were added in 3.6 ml of LB medium and grown at 37°C in the presence or absence of telithromycin until the optical density of the control culture (grown in the absence of telithromycin) reached the value 0.700 at 560 nm. From the curves obtained, the IC_{50} value for each strain was estimated as the concentration of telithromycin that is required to bring the corresponding curve optical density down to point half way between the value 0.700 and bottom plateau.

Statistics

All data shown in Tables or kinetic diagrams denote mean values obtained from three independently performed experiments. Data variability was determined by ANOVA, while significant differences between mean values were measured by the *F*-Scheffé test (SPSS program 17.0 for Windows).

RESULTS

Telithromycin behaves as a slow-binding ligand of ribosomes, following a two-step mechanism

Previous studies have showed that tylosin inhibits the AcPhe-puromycin synthesis at 4.5 mM $Mg^{2+}$and 150 mM NH_4^+, following a two-step mechanism (4,12). In contrast, as shown in Figure 2A, telithromycin fails to inhibit this model reaction. This renders the kinetic analysis of telithromycin interaction with complex C impossible, if the PTase activity is monitored. Nevertheless, tylosin and telithromycin exhibit an overlapping footprinting pattern predicting that telithromycin competes with tylosin for binding to complex C. Indeed, as shown in Figure 2B, complex C addition in a solution containing tylosin at 4 µM and telithromycin at increasing concentrations results in non-linear inactivation curves, whose initial slopes vary as a function of telithromycin concentration. At high concentrations of telithromycin (>10 µM), the inactivation of complex C by tylosin is entirely reversed. Interestingly, when complex C is preincubated for 15 min with telithromycin

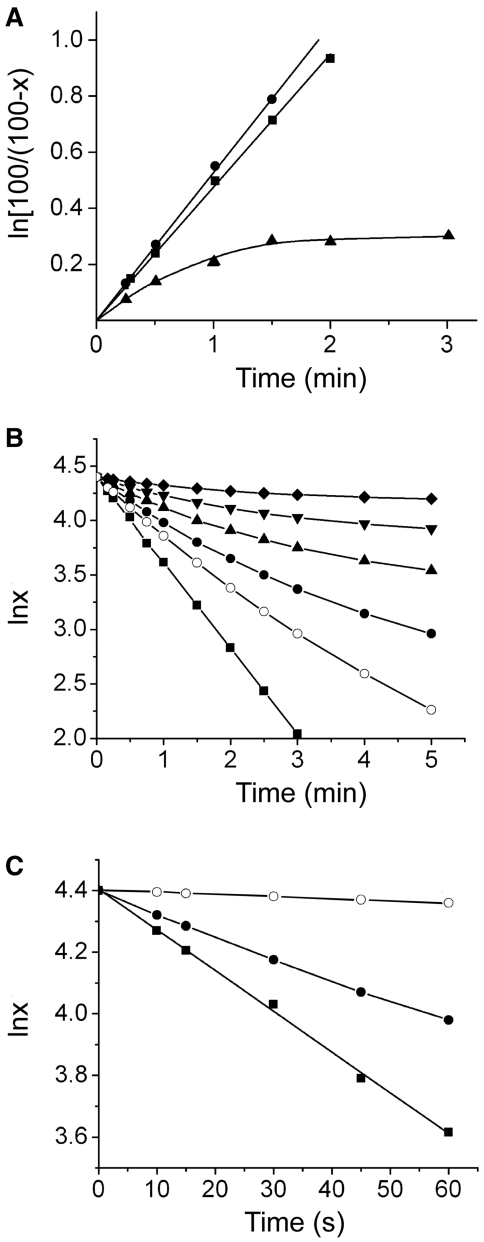

Figure 2. Kinetics of telithromycin. (**A**) AcPhe-puromycin synthesis in the absence or presence of antibiotics; complex C prepared from *E. coli* ribosomes was reacted in buffer A at 25°C with 200 µM puromycin alone (filled circle), or with a mixture containing both 200 µM puromycin and 2 µM telithromycin (filled square), or 200 µM puromycin and 2 µM tylosin (filled triangle). (**B**) effect of telithromycin on the inactivation of complex C by tylosin; complex C was incubated in buffer A with 4 µM tylosin alone (filled square), or with a mixture containing 4 µM tylosin and telithromycin at 0.5 (open circle), 1 (filled circle), 2 (filled triangle), 4 (filled inverted triangle), and 10 µM (filled rhombus). The percentage of the complex C input remaining active, *x*, was determined with 2 mM puromycin (25°C, 2 min). (**C**) pre-incubation effect; complex C was incubated in buffer A with 4 µM tylosin alone (filled square), or with a mixture containing 4 µM tylosin and telithromycin at 1 µM (filled circle), or first pre-incubated with 1 µM telithromycin for 15 min, and then reacted with 4 µM tylosin for the time intervals indicated (open circle). The *x* value was determined as stated in (B).

before adding tylosin, the protection of complex C against tylosin becomes stronger (preincubation effect; Figure 2C). This inactivation pattern is reminiscent of that observed in a previous study regarding erythromycin binding (4), and strongly suggests adopting a similar kinetic model, which here is represented by Scheme 1. The values of $k_{on,T}$, $k_{off,T}$ and K_T calculated by kinetic analysis are shown in Table 1 (for kinetic Equations and data processing, see Supplementary Data). A value of $8.33 \times 10^{-3}\,min^{-1}$ estimated for $k_{off,T}$ from the slope of the diagram shown in Figure 3, is quite similar to that presented in Table 1. A second information drawn from Figure 3 is that complex C regeneration from complex C*T gives a simple first-order time plot, suggesting one molecule of telithromycin bound per *E. coli* ribosome.

By repeating experiments in the presence of 100 μM spermine or in an optimized polyamine buffer (50 μM spermine and 2 mM spermidine; ref. 37), we observed that the K_T value undergoes at least a 3-fold increase, whereas $k_{on,T}$ value and the isomerization constant $k_{on,T}/\ k_{off,T}$ are decreased by 83 and 64%, respectively (Table 1).

Regarding the impact of mutations on telithromycin binding, U2609C and L22: Δ82–84 show the stronger effects. Both mutations cause a 20-fold enhancement on the overall affinity constant K^*_T, by decreasing the $k_{on,T}$ value and increasing the $k_{off,T}$ value. Instead, both mutations hardly affect the K_T value. Mutation U754A exhibits a less pronounced effect, doubling the value of $k_{off,T}$ constant, while mutation Lys63Glu in L4 does not essentially affect telithromycin binding (Table 1). Evidence in corroboration was sought in experiments assessing the *in vivo* sensitivity of *E. coli* strains against telithromycin. As shown in Table 2, the IC_{50} values measured in wild-type cells or mutants U754A and L4: Lys63Glu are much smaller than in U2609C or L22: Δ82–84 mutants.

Footprinting analysis of CT and C*T complexes

The first step of telithromycin binding to complex C is presented by a bimolecular reaction. Therefore, to footprint the CT complex, telithromycin at concentration $50 \times K_T$ and complex C at 100 nM were incubated at 25°C for 5 s. Since the equilibrium $C + T \rightleftharpoons CT$ is established instantaneously while the subsequent isomerization step proceeds slowly, the species mainly produced during this time interval is complex CT (>97%). By longer exposure of complex C to telithromycin ($8 \times t_{1/2}$), the high value, 58.93, for the isomerization constant of the second step favors the formation of C*T complex (>98%). Next to their formation, complexes CT and C*T were probed with DMS, CMCT or kethoxal. Noteworthy, the chemical probes used react with accessible bases within milliseconds (38). Representative autoradiograms obtained by primer extension analysis in helix 35 of domain II and the central loop of domain V of 23S rRNA are shown in Figure 4, while relative reactivities of the modified nucleotides are summarized in Table 3. To assess the footprinting changes relative to the rest of neighboring 23S rRNA areas, larger regions of the scanned sequences are given in Supplementary Figures S1 and S2. Telithromycin in the CT binding state and in the absence of polyamines strongly protects A2058, A2059 and to a lesser degree G2505, C2611, A752, A789 and U790. In contrast, it causes an enhancement in the susceptibility of A2062 to DMS. In the C*T binding state, the protection effects at A789 and U790 soften, the protection at A752 enhances, while a new protection appears on U2609.

Spermine, either alone or in a mixture with spermidine, reduces the protection of all nucleotides involved in telithromycin binding, in particular of U2609 and A752 in complex C*T, and of A2058 in both complexes. Interestingly, in the presence of polyamines, the reactivity of C2611 is lost in either complex. This phenomenon, also observed previously (4,12), may be related to a stabilization effect that polyamines exert on the C2611/G2057 base pair at low concentrations of Mg^{2+}.

DISCUSSION

Crystallographic studies of ribosomal subunits complexed with telithromycin presents an extended panel of detailed view of the ribosome–drug interactions at atomic resolution. Nevertheless, these studies often use fairly artificial complexes that do not reproduce the ionic cell-environment, and worse still provide only a snapshot of telithromycin binding process. In the present

Table 1. Equilibrium and kinetic constants derived from analysis of the telithromycin binding to complex C[a]

Constant (unit)	Ionic conditions						
	4.5 mM Mg^{2+}, 150 mM NH_4^+					4.5 mM Mg^{2+}, 150 mM NH_4^+ 100 μM spermine	4.5 mM Mg^{2+} 150 mM NH_4^+ 50 μM spermine 2 mM spermidine
	Wild-type	U2609C	U754A	L22: Δ82–84	L4: Lys63Glu	Wild-type	Wild-type
K_T (nM)	500 ± 44	536 ± 43	604 ± 45	530 ± 42	470 ± 48	2500 ± 185	1714 ± 13
$k_{on,T}$ (min^{-1})	0.480 ± 0.040	0.103 ± 0.008	0.430 ± 0.040	0.046 ± 0.005	0.290 ± 0.050	0.078 ± 0.006	0.082 ± 0.006
$k_{off,T}$ (min^{-1})	0.0082 ± 0,0006	0.0395 ± 0.0031	0.0166 ± 0.0014	0.0300 ± 0.003	0.0076 ± 0.0008	0.0029 ± 0.0002	0.0038 ± 0.0001
$k_{on,T}/\ k_{off,T}$	58.93 ± 6.52	2.61 ± 0.29	25.90 ± 3.25	1.53 ± 0.22	38.16 ± 7.71	26.90 ± 2.77	21.58 ± 1.90
K^*_T (nM)	8.33 ± 1.16	148.00 ± 18.92	22.60 ± 3.22	210.00 ± 30.93	12.00 ± 2.67	91.40 ± 11.24	75.70 ± 8.80

[a]Data represent the mean ± SE values obtained from three independently performed experiments.

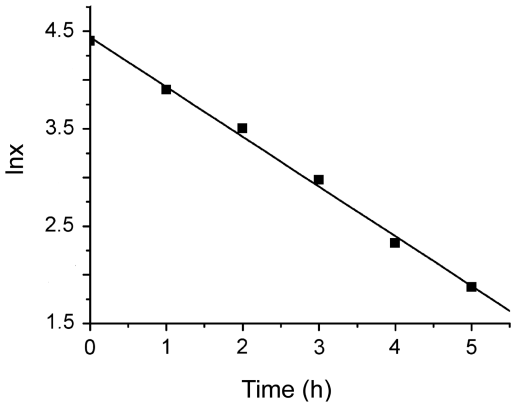

Figure 3. Dissociation of telithromycin from complex C*T; complex C*T formed by incubating complex C in buffer A with 2.5 μM telithromycin at 25°C for 15 min was adsorbed by filtration on a cellulose nitrate filter, exposed to 5 ml of 4 μM tylosin in buffer A for the time intervals indicated, and the percentage of complex C*T remaining active, *x*, was titrated with puromycin.

Table 2. Half maximal inhibitory concentrations (IC_{50}) for telithromycin, indicating how much of the drug is needed to inhibit the growth of wild-type *E. coli* cells or mutants by half[a]

Mutation	IC_{50} (μg/ml)
None	4.0 ± 0.8
L4: Lys63Glu	12.0 ± 2.1*
U754A	14.8 ± 2.5*
U2609C	41.6 ± 4.3*, **
L22: Δ82–84	50.0 ± 6.5*, **

[a]Data represent the mean ± SE values obtained from three independently performed experiments.
*Significantly different in relation to wild-type cells ($P < 0.05$); **Significantly different in relation to L4: Lys63Glu or U754A mutants ($P < 0.05$).

study, kinetic analysis combined with chemical probing at discrete time-intervals following mixing the ribosome with the drug give us the opportunity to investigate the entire course of telithromycin binding to *E. coli* functional ribosomes, under near physiological ionic conditions.

Our results indicate that telithromycin interacts with a model post-translocation ribosomal complex C, at 4.5 mM Mg^{2+} and 150 mM NH_4^+, via a two-step mechanism. Supportive evidence for the consistency of this model with our kinetic results is provided by the following findings: first, the initial slopes of the inactivation curves in Figure 2B vary as a function of the telithromycin concentration, second, the *k* versus [telithromycin] plot is represented by a rectangular hyperbolic curve (data not shown) and, third, the potency of telithromycin to reverse the inactivation of complex C by tylosin increases if complex C is pre-incubated with telithromycin before adding tylosin (pre-incubation effect; Figure 2C). In addition, the apparent association rate constant of telithromycin binding, $(k_{on,T} + k_{off,T})/K_T$, equals $1.6 \times 10^4 M^{-1}s^{-1}$ a value two orders of magnitude below the upper limit set for the characterization of a drug as a slow binding, slowly reversible ligand (35). Moreover, the value of the isomerization constant, $k_{on,T} / k_{off,T}$, is much higher than 1. Based on these results, we suggest that an initial and rapidly equilibrated step is followed by a slow isomerization step which facilitates accommodation of the drug at its final position. Binding of telithromycin at the initial and final positions is mutually exclusive, which means that only one molecule of telithromycin binds per ribosome at a time. A similar conclusion is also drawn by regeneration of complex C from complex C*T, which follows a linear first-order time-plot (Figure 3). A drug:ribosome stoichiometry equal to one has also been determined previously, by titrating the ribosomal binding site for telithromycin via footprinting analysis (18).

At 4.5 mM Mg^{2+} and 150 mM NH_4^+, telithromycin shows a slightly higher overall affinity for the complex C target than does erythromycin (4), but displays a significantly lower affinity than those of azithromycin (12) and 16-membered lactone ring macrolides (4,29). A similar order of potency has also been assigned to these antibiotics on the basis of K_D values calculated by fluorescence polarization (39). Binding of telithromycin to complex C is affected by polyamines at both steps; K_T value becomes over 3-fold higher, whereas the isomerization constant undergoes a 50% reduction. Although the value of K_T* becomes 10-fold higher, telithromycin retains its relative potency compared to the other antibiotics, because parallel alterations are caused by the polyamine buffer in the kinetic constants of the latter drugs (4,12,29).

The slow dissociation of complex C*T ($k_{off,T} = 0.0082$/min) acquires pharmaceutical significance. Binding of telithromycin at the exit tunnel constriction jams the tunnel, causing arrest to protein synthesis, a fact eventually leading to drop off of peptidyl-tRNA from the ribosome (3). Since $k_{off,T}$ is 10 times lower than the rate constant for drop off calculated by Lovmar *et al.* (3), it is predicted that telithromycin at saturating concentrations might completely shut down the elongation of nascent peptides. Instead, erythromycin has a k_{off} value almost equal to the rate constant for drop off (4), a fact rendering dissociation of erythromycin equally probable. Consequently, sensitivity of the ribosome against erythromycin is less pronounced. There is also an apparent relationship between k_{off} value and post-antibiotic effect (PAE) (40), in that telithromycin has slower dissociation rate and longer PAE compared with erythromycin, leading in other words to longer persistent antibacterial effects after drug removal from the growth medium.

The structural characterization of complexes CT and C*T was obtained by footprinting analysis. As shown in Table 3, telithromycin binding at the initial site (complex CT) protects G2505, nucleotides clustered around a hydrophobic crevice (nts: G2057- A2059) placed at the entrance to the exit tunnel, and nucleotides in domain II of 23 S rRNA positioned further down the peptide exit tunnel (nts: A752, A789, U790). Meanwhile, the reactivity of A2062 against DMS becomes stronger. The footprinting pattern of complex CT does not

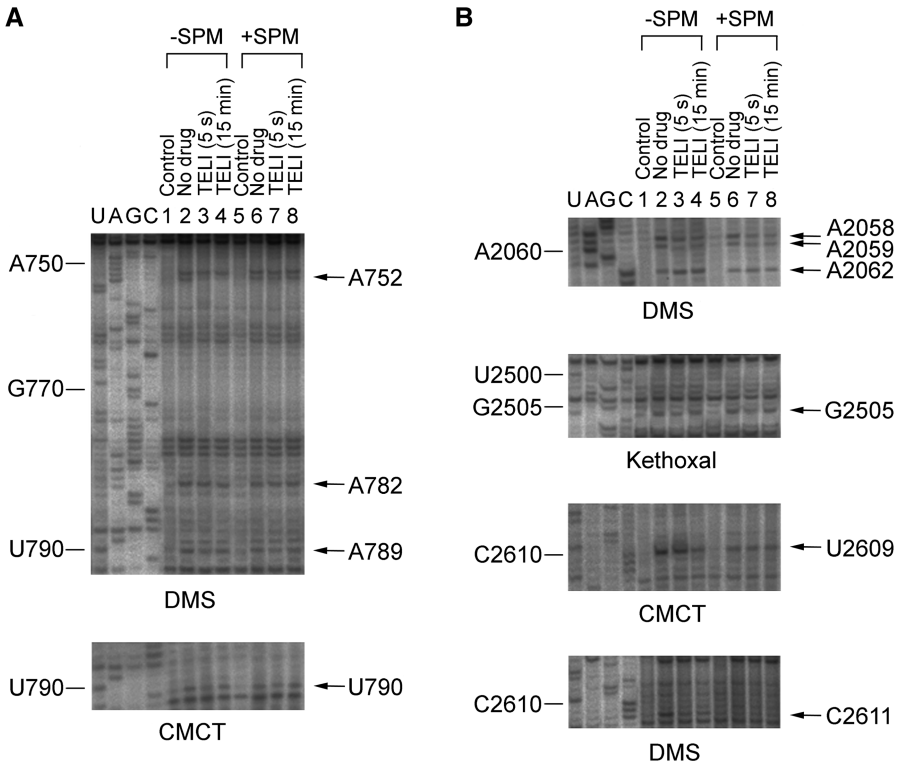

Figure 4. Protections in nucleotides of 23S rRNA from chemical probes, caused by binding of telithromycin to complex C prepared from *E. coli* ribosomes. (**A**) protections in domain II of 23S rRNA; complex C was incubated in the absence or presence of telithromycin in buffer B (lanes 1–4) or in the same solution also containing 100 μM spermine (lanes 5–8). The resulting complexes were then probed with DMS or CMCT. U, A, G and C, dideoxy sequencing lanes; lane 2 and 6, complex C probed in the absence of telithromycin; lanes 3 and 7, complex C pre-incubated with telithromycin for 5 s and then probed; lanes 4 and 8, complex C pre-incubated with telithromycin for 15 min and then probed. (**B**) protection in the central loop of domain V of 23 S rRNA; incubation of complex C with telithromycin was carried out as in panel A. Samples were then modified with DMS, kethoxal, or CMCT, and analyzed as in panel A. Numbering of nucleotides for the sequencing lanes is indicated at the left of each panel, while nucleotides with reactivity to probes along with reference bands are shown by arrows. Teli, telithromycin.

Table 3. Footprinting of the telithromycin binding sites in the initial (CT) and the final (C*T) binding site[a]

23 S rRNA residue	Ionic conditions					
	4.5 mM Mg^{2+} 150 mM NH_4^+			4.5 mM Mg^{2+} 150 mM NH_4^+ 100 μM spermine		
	C	CT	C*T	C	CT	C*T
A752	1	0.65 ± 0.05*	0.30 ± 0.02*, **	1	0.75 ± 0.05*	0.87 ± 0.07*
A789	1	0.78 ± 0.07*	0.89 ± 0.08	1	0.82 ± 0.08*	0.93 ± 0.08
U790	1	0.60 ± 0.07*	0.85 ± 0.08*, **	1	0.70 ± 0.07*	0.93 ± 0.08**
A2058	1	0.20 ± 0.02*	0.25 ± 0.03*	1	0.30 ± 0.01*	0.38 ± 0.02*, **
A2059	1	0.38 ± 0.03*	0.42 ± 0.03*	1	0.45 ± 0.05*	0.57 ± 0.03*, **
A2062	1	1.33 ± 0.18*	1.28 ± 0.15*	1	1.20 ± 0.14	1.15 ± 0.14
G2505	1	0.65 ± 0.09*	0.78 ± 0.11*	1	0.72 ± 0.07*	0.85 ± 0.06*
U2609	1	0.95 ± 0.07	0.72 ± 0.04*, **	1	0.97 ± 0.07	0.90 ± 0.08
C2611	1	0.60 ± 0.09*	0.60 ± 0.08*	1	0.98 ± 0.05	0.97 ± 0.05

[a]Relative reactivity of nucleotides denotes the ratio between the intensity of a band of interest and the intensity of the corresponding band in the control lane (complex C). Only residues, whose reactivity changes upon exposure to telithromycin, are shown.
*Significantly different in relation to C for the same ionic conditions ($P < 0.05$); **Significantly different in relation to CT for the same ionic conditions ($P < 0.05$)

significantly differ to that published for telithromycin–ribosome interaction by other groups (18,20), except for the absence of protection at U2609, the appearance of new protections at A789 and U790, and the relatively weaker protection at A752. It correlates well with crystallographic data obtained with *D. radiodurans* 50S ribosomal subunit in complex with telithromycin (26). In this crystallographic study, the alkyl–aryl arm of telithromycin does not orient toward U2609, but inserts into a groove formed by nucleotides A751, A789 and U790 within

domain II of 23S rRNA. Nevertheless, there are a number of differences in the sequence and structures between *D. radiodurans* and *E. coli* in this region of 23S rRNA, and a putative rotation of U790 from position (a) to position (b) upon binding of telithromycin to the initial site should be assumed to explain a stacking interaction of the telithromycin side chain against the base of U790 (Figure 5). The lack of protection effects at U2609 does not support the proposal that the formation of a base pair between U2609 and A752 is induced upon initial binding of telithromycin to the ribosome (30). Such a pairing, detected by recent crystallographic studies in *E. coli* ribosomes complexed with telithromycin (31), might be a delayed event induced by conformational changes occurring during the next isomerization step (see below). Corroborative evidence is coming from kinetic studies involving ribosomes bearing mutation U2609C; no impact of this mutation on K_T value is evident (Table 1). In the presence of spermine, a general softening of protections is notable. This may be due to one or more of the following reasons: (i) inactivation of the chemical probes by freely circulating spermine (41); (ii) competition between spermine and chemical probes for binding to certain residues of 23S rRNA; and (iii) conformation changes induced by spermine and leading to inhibition of telithromycin binding to ribosomes. Although we cannot completely disregard the two first possibilities, kinetic results are tempting us to adopt the third hypothesis. As shown in Table 1, the presence of spermine causes a 5-fold decrease in the affinity of telithromycin for the initial site. As indicated before, spermine is capable of binding to ribosomal regions implicated in telithromycin accommodation, and induces conformational changes on the ribosome (42). Similar observations were obtained when an optimized mixture of spermine and spermidine was used instead of spermine alone.

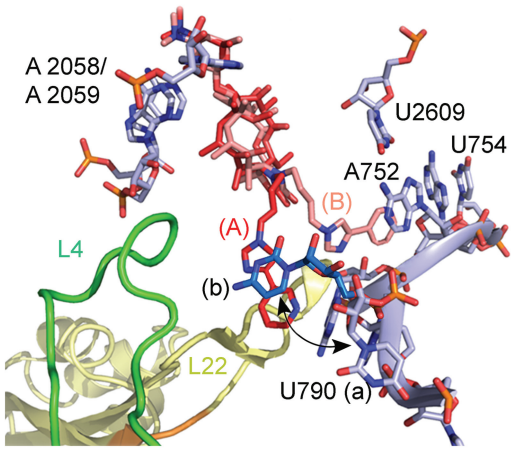

Figure 5. Stepwise binding of telithromycin to *E. coli* ribosomes. 50S subunit cross-section showing the upper segment of the peptide exit tunnel. (A) and (B), models of telithromycin binding at the initial and final site, respectively. A putative rotation of U790 from position (a) to position (b) upon binding of telithromycin to the initial site is indicated by a double arrow. The subunit structure was drawn from the coordinates of Schuwirth *et al.* (46), while the modeling of telithromycin binding was derived from footprinting results of the present study.

The footprinting pattern of complex C*T resembles better those published by others and generally correlates well with recent crystallographic data obtained with ribosomes from *T. thermophilus* and *E. coli*, complexed with telithromycin (31,32). This may be due to the fact that both footprinting and crystallographic analyses have been performed by incubating ribosomes with high concentrations of telithromycin for prolonged time. Accommodation of telithromycin at its final position weakens the contacts with nucleotides A789, U790 and G2505, but favors drug interactions with A752 and U2609 (Table 3). In excellent agreement, U754A destabilizes complex C*T (Table 1); U754 base pairs with A743, and therefore, U754A may disrupt helix 35 in domain II of 23S rRNA, thus indirectly affecting the conformation of A752 which contacts telithromycin (31,32). In addition, U2609C mutation prevents C*T formation by hindering the shift of telithromycin to the high affinity site and destabilizing the final complex C*T. Similarly, deletion of three amino acids in the finger-like β-hairpin of ribosomal protein L22 disfavors the formation of complex C*T, without affecting the first step of telithromycin binding (Table 1). In contrast, mutation Lys63Glu in a finger-like extension of ribosomal protein L4 does not significantly alter the kinetics at both steps of telithromycin binding. However, the same mutation, causes a 380-fold reduction in the dissociation constant (K_D) for erythromycin–ribosome complex, rendering this mutant resistant to erythromycin (43). The tips of the fingers from L22 and L4 along with rRNA residues form what appears to be a constriction at the upper segment of the exit tunnel, near the PTase center (44). Namely, the finger-like extension of L4 projects towards the tunnel wall, where the hydrophobic crevice G2057-A2058-A2059 is located. The tip of L22 finger-like β-hairpin is orientated towards the opposite side of the tunnel wall and interacts with helix 35 in domain II of 23S rRNA (Figure 5). We suppose that deletion Δ82–84 in L22 results in a change of the overall orientation of the tip of hairpin, which in turn perturbs the interaction of the hairpin-tip with helix 35, leading finally to disruption of the A752–U2609 base pair. Cryo-electron microscopy (cryo-EM) data have suggested a broadening of the peptide exit tunnel by the L22: Δ82–84 mutation (45). Therefore, one could hypothesize that drug-dependent blockage of the nascent peptide chain progression through the exit tunnel may be by-passed by tunnel widening due to the L22: Δ82–84 mutation. Instead, our results show a 25-fold increase in the overall dissociation constant K^*_T, a 10-fold reduction in association rate constant $k_{on,T}$, and about 4-fold enhancement in dissociation rate constant $k_{off,T}$ by the L22: Δ82–84 mutation. These kinetic changes justify that telithromycin resistance is likely conferred by perturbation of the drug kinetic properties, making the nascent chain by-pass model less convincing. In corroboration of this argument, crystallographic data have suggested that the apparent broadening of the exit tunnel seen by cryo-EM is due to the flexibility of the mutant L22 loop rather than to a widening of the tunnel (27). Polyamines exert again an inhibitory effect on the formation and stability of complex C*T (Table 1).

Our results reconcile a large body of experimental data, and suggest a two-step drug binding mechanism, whereby telithromycin is recognized by an initial subsite of the *E.coli* ribosome to allow the drug to sequentially progress toward a final favorable orientation (Figure 5). While the initial orientation is reminiscent of that crystallographically seen in *D. radiodurans*, accommodation at the final position orientates the extended arm of telithromycin in such a way, so that the aryl-end of the extension stacks on the A752–U2609 base pair formed during the shift of the drug from the initial to the final position. In contrast, the macrolactone portion remains at essentially the same position, except for a slight movement uncovered by small alterations in protection of nucleotides A2058, A2059, A2062 and G2505. Although not accurate enough for proper quantification, these small changes suggest that telithromycin may tolerate some perturbations to the primary binding site by picking up new binding from the stacking interactions of the alkyl–aryl side chain. Finally, combined with crystallographic data, our results support the notion that the precise placement of a drug molecule can vary not only in ribosomes of different species, but also in the same species under different ionic conditions or at different phases of its accommodation with the ribosome.

SUPPLEMENTARY DATA

Supplementary Data are available at NAR Online: Supplementary Figures S1 and S2, and Supplementary Data.

ACKNOWLEDGMENTS

We thank Dr Constantinos Stathopoulos for critical reading of the manuscript, Dr Daniel Wilson for creating Figure 5, and Drs A.S. Mankin and S.T. Gregory for providing us with mutated strains of *E. coli*. Also, we wish to thank Sanofi-Aventis Inc. for telithromycin supply and covering the expenses of publication.

FUNDING

Research Committee of the University of Patras (Programme K. Karatheodoris: B115 grant to D.L.K). Funding for open access charge: Sanofi-Aventis A.E.B.E., Athens, Greece.

Conflict of interest statement. None declared.

REFERENCES

1. Ma,X. and Ma,S. (2011) Significant breakthroughs in search for anti-infectious agents derived from erythromycin A. *Curr. Med. Chem.*, **18**, 1993–2015.
2. Wilson,D.N. (2009) The A-Z of bacterial translation inhibitors. *Crit. Rev. Biochem. Mol. Biol.*, **44**, 393–433.
3. Lovmar,M., Tenson,T. and Ehrenberg,M. (2004) Kinetics of macrolide action: the josamycin and erythromycin cases. *J. Biol. Chem.*, **279**, 53506–53515.
4. Petropoulos,A.D., Kouvela,E.C., Dinos,G.P. and Kalpaxis,D.L. (2008) Stepwise binding of tylosin and erythromycin to *Escherichia coli* ribosomes, characterized by kinetic and footprinting analysis. *J. Biol. Chem.*, **283**, 4756–4765.
5. Pestka,S. (1974) Binding of [^{14}C]erythromycin to *Escherichia coli* ribosomes. *Antimicrob. Agents Chemother.*, **6**, 474–478.
6. Di Giambattista,M., Engelborghs,Y., Nyssen,E. and Cocito,C. (1987) Kinetics of binding of macrolides, lincosamides, and synergimycins to ribosomes. *J. Biol. Chem.*, **262**, 8591–8597.
7. Douthwaite,S., Hansen,L.H. and Mauvais,P. (2000) Macrolide-ketolide inhibition of MLS-resistant ribosomes is improved by alternative drug interaction with domain II of 23S rRNA. *Mol. Microbiol.*, **36**, 183–193.
8. Langlois,R., Lee,C.C., Cantor,C.R., Vince,R. and Pestka,S. (1976) The distance between two functionally significant regions of the 50 S *Escherichia coli* ribosome: the erythromycin binding site and proteins L7/L12. *J. Mol. Biol.*, **106**, 297–313.
9. Dinos,G., Synetos,D. and Coutsogeorgopoulos,C. (1993) Interaction between the antibiotic spiramycin and a ribosomal complex active in peptide bond formation. *Biochemistry*, **32**, 10638–10647.
10. Dinos,G.P. and Kalpaxis,D.L. (2000) Kinetic studies on the interaction between a ribosomal complex active in peptide bond formation and the macrolide antibiotics tylosin and erythromycin. *Biochemistry*, **39**, 11621–11628.
11. Dinos,G.P., Connell,S.R., Nierhaus,K.H. and Kalpaxis,D.L. (2003) Erythromycin, roxithromycin, and clarithromycin: use of slow-binding kinetics to compare their *in vitro* interaction with a bacterial ribosomal complex active in peptide bond formation. *Mol. Pharmacol.*, **63**, 617–623.
12. Petropoulos,A.D., Kouvela,E.C., Starosta,A.L., Wilson,D.N., Dinos,G.P. and Kalpaxis,D.L. (2009) Time-resolved binding of azithromycin to *Escherichia coli* ribosomes. *J. Mol. Biol.*, **385**, 1179–1192.
13. Bertho,G., Gharbi-Benarous,J., Delaforge,M. and Girault,J.P. (1998) Transferred nuclear Overhauser effect study of macrolide-ribosome interactions: correlation between antibiotic activities and bound conformations. *Bioorg. Med. Chem.*, **6**, 209–221.
14. Novak,P., Tatić,I., Tepes,P., Kostrun,S. and Barber,J. (2006) Systematic approach to understanding macrolide-ribosome interactions: NMR and modeling studies of oleandomycin and its derivatives. *J. Phys. Chem.*, **110**, 572–579.
15. Bryskier,A. (2000) Ketolides-telithromycin, an example of a new class of antibacterial agents. *Clin. Microbiol. Infect.*, **6**, 661–669.
16. Ackermann,G. and Rodloff,A.C. (2003) Drugs of the 21st century: telithromycin (HMR 3647)-the first ketolide. *J. Antimicrob. Chemother.*, **51**, 497–511.
17. Brown,S.D. (2008) Benefit-risk assessment of telithromycin in the treatment of community-acquired pneumonia. *Drug Saf.*, **31**, 561–575.
18. Hansen,L.H., Mauvais,P. and Douthwaite,S. (1999) The macrolide-ketolide antibiotic binding site is formed by structures in domains II and V of 23S ribosomal RNA. *Mol. Microbiol.*, **31**, 623–631.
19. Tait-Kamradt,A., Davies,T., Cronan,M., Jacobs,M.R., Appelbaum,P.C. and Sutcliffe,J. (2000) Mutations in 23S rRNA and ribosomal protein L4 account for resistance in pneumococcal strains selected *in vitro* by macrolide passage. *Antimicrob. Agents Chemother.*, **44**, 2118–2125.
20. Garza-Ramos,G., Xiong,L., Zhong,P. and Mankin,A. (2001) Binding site of macrolide antibiotics on the ribosome: new resistance mutation identifies a specific interaction of ketolides with rRNA. *J. Bacteriol.*, **183**, 6898–6907.
21. Canu,A., Malbruny,B., Coquemont,M., Davies,T.A., Appelbaum,P.C. and Leclercq,R. (2002) Diversity of ribosomal mutations conferring resistance to macrolides, clindamycin, streptogramin, and telithromycin in *Streptococcus pneumoniae*. *Antimicrob. Agents Chemother.*, **46**, 125–131.
22. Novotny,G.W., Jakobsen,L., Andersen,N.M., Poehlsgaard,J. and Douthwaite,S. (2004) Ketolide antimicrobial activity persists after disruption of interactions with domain II of 23S rRNA. *Antimicrob. Agents Chemother.*, **48**, 3677–3683.

23. Franceschi,F., Kanyo,Z., Sherer,E.C. and Sutcliffe,J. (2004) Macrolide resistance from the ribosome perspective. *Curr. Drug Targets Infect. Disord.*, **4**, 177–191.
24. Pfister,P., Jenni,S., Poehlsgaard,J., Thomas,A., Douthwaite,S., Ban,N. and Böttger,E.C. (2004) The structural basis of macrolide-ribosome binding assessed using mutagenesis of 23S rRNA positions 2058 and 2059. *J. Mol. Biol.*, **342**, 1569–1581.
25. Pfister,P., Corti,N., Hobbie,S., Bruell,C., Zarivach,R., Yonath,A. and Böttger,E.C. (2005) 23S rRNA base pair 2057–2611 determines ketolide susceptibility and fitness cost of the macrolide resistance mutation 2058A→G. *Proc. Natl Acad. Sci. U S A.*, **102**, 5180–5185.
26. Berisio,R., Harms,J., Schluenzen,F., Zarivach,R., Hansen,H.A., Fucini,P. and Yonath,A. (2003) Structural insight into the antibiotic action of telithromycin against resistant mutants. *J. Bacteriol.*, **185**, 4276–4279.
27. Tu,D., Blaha,G., Moore,P.B. and Steitz,T.A. (2005) Structures of MLSBK antibiotics bound to mutated large ribosomal subunits provide a structural explanation for resistance. *Cell*, **121**, 257–270.
28. Bertho,G., Gharbi-Benarous,J., Delaforge,M., Lang,C., Parent,A. and Girault,J.P. (1998) Conformational analysis of ketolide, conformations of RU 004 in solution and bound to bacterial ribosomes. *J. Med. Chem.*, **41**, 3373–3386.
29. Petropoulos,A.D., Xaplanteri,M.A., Dinos,G.P., Wilson,D.N. and Kalpaxis,D.L. (2004) Polyamines affect diversely the antibiotic potency: insight gained from kinetic studies of the blasticidin S and spiramycin interactions with functional ribosomes. *J. Biol. Chem.*, **279**, 26518–26525.
30. Wilson,D.N., Harms,J.M., Nierhaus,K.H., Schlünzen,F. and Fucini,P. (2005) Species-specific antibiotic-ribosome interactions: implications for drug development. *Biol. Chem.*, **386**, 1239–1252.
31. Dunkle,J.A., Xiong,L., Mankin,A.S. and Cate,J.H. (2010) Structures of the *Escherichia coli* ribosome with antibiotics bound near the peptidyl transferase center explain spectra of drug action. *Proc. Natl Acad. Sci. USA*, **107**, 17152–17157.
32. Bulkley,D., Innis,C.A., Blaha,G. and Steitz,T.A. (2010) Revisiting the structures of several antibiotics bound to the bacterial ribosome. *Proc. Natl Acad. Sci. USA*, **107**, 17158–17163.
33. Gregory,S.T. and Dahlberg,A.E. (1999) Mutations in the conserved P loop perturb the conformation of two structural elements in the peptidyl transferase center of 23S ribosomal RNA. *J. Mol. Biol.*, **285**, 1475–1483.
34. Dinos,G., Wilson,D.N., Teraoka,Y., Szaflarski,W., Fucini,P., Kalpaxis,D. and Nierhaus,K.H. (2004) Dissecting the ribosomal inhibition mechanisms of edeine and pactamycin: the universally conserved residues G693 and C795 regulate P-site RNA binding. *Mol. Cell*, **13**, 113–124.
35. Morrison,J.F. and Walsh,C.T. (1988) The behavior and significance of slow-binding enzyme inhibitors. *Adv. Enzymol. Relat. Areas Mol. Biol.*, **61**, 201–301.
36. Stern,S., Moazed,D. and Noller,H.F. (1988) Structural analysis of RNA using chemical and enzymatic probing monitored by primer extension. *Methods Enzymol.*, **164**, 481–489.
37. Bartetzko,A. and Nierhaus,K.H. (1988) Mg^{2+}/NH_4^+/polyamine system for polyuridine-dependent polyphenylalanine synthesis with near *in vivo* characteristics. *Methods Enzymol.*, **164**, 650–658.
38. Fabbretti,A., Milon,P., Giuliodori,A.M., Gualerzi,C.O. and Pon,C.L. (2007) Real-time dynamics of ribosome-ligand interaction by time-resolved chemical probing methods. *Methods Enzymol.*, **430**, 45–58.
39. Yan,K., Hunt,E., Berge,J., May,E., Copeland,R.A. and Gontarek,R.R. (2005) Fluorescence polarization method to characterize macrolide-ribosome interactions. *Antimicrob. Agents Chemother.*, **49**, 3367–3372.
40. Nilius,A.M. and Ma,Z. (2002) Ketolides: the future of the macrolides? *Curr. Opin. Pharmacol.*, **2**, 493–500.
41. Ehresmann,C., Baudin,F., Mougel,M., Romby,P., Ebel,J.P. and Ehresmann,B. (1987) Probing the structure of RNAs in solution. *Nucleic Acids Res.*, **15**, 9109–9128.
42. Xaplanteri,M.A., Petropoulos,A.D., Dinos,G.P. and Kalpaxis,D.L. (2005) Localization of spermine binding sites in 23S rRNA by photoaffinity labeling: parsing the spermine contribution to ribosomal 50S subunit functions. *Nucleic Acids Res.*, **33**, 2792–2805.
43. Lovmar,M., Nilsson,K., Lukk,E., Vimberg,V., Tenson,T. and Ehrenberg,M. (2009) Erythromycin resistance by L4/L22 mutations and resistance masking by drug efflux pump deficiency. *EMBO J.*, **28**, 736–744.
44. Jenni,S. and Ban,N. (2003) The chemistry of protein synthesis and voyage through the ribosomal tunnel. *Curr. Opin. Struct. Biol.*, **13**, 212–219.
45. Gabashvili,I.S., Gregory,S.T., Valle,M., Grassucci,R., Worbs,M., Wahl,M.C., Dahlberg,A.E. and Frank,J. (2001) The polypeptide tunnel system in the ribosome and its gating in erythromycin resistance mutants of L4 and L22. *Mol. Cell*, **8**, 181–188.
46. Schuwirth,B.S., Borovinskaya,M.A., Hau,C.W., Zhang,W., Vila-Sanjurjo,A., Holton,J.M. and Cate,J.H. (2005) Structures of the bacterial ribosome at 3.5 A resolution. *Science*, **310**, 827–834.